Proceedings of 20th International Congress on Acoustics, ICA 2010

23-27 August 2010, Sydney, Australia

Studies on Substructure FMBEM and Direct Mixed-body FMBEM for Acoustic Performance Prediction of Reactive Mufflers

Xiaobing Cui, Zhenlin Ji

College of Power and Energy Engineering, Harbin Engineering University, Harbin, China

PACS: 43.20.RZ

ABSTRACT

Due to the advantage of fast computation and drastic memory saving in solving the large-scale problems, the FMBEM has been developed rapidly in recent years. But it is hard to be employed directly to the acoustic computation of mufflers with complex structures (such as mufflers with extended inlet/outlet tubes or perforated tubes). Two approaches for FMBEM (the substructure FMBEM and the direct mixed-body FMBEM) are investigated and applied to predict the acoustic performance of mufflers in the present paper. For the substructure FMBEM, the interior acoustic domain is divided into several subdomains first, and then the FMBEM is applied to each domain. The direct mixed-body FMBEM may deal with the muffler with complex internal geometry without dividing subdomains, which is achieved by summing up all the integral equations in different zones and then adding the hypersingular integral equations at interfaces. The transmission loss of expansion chamber mufflers with extended tubes are predicted by using the two approaches and verified by the experimental data. The computational time is compared, and the computational accuracy and efficiency are discussed for the two approaches.

INTRODUCTION

Mufflers are widely used in the intake and exhaust systems of internal combustion engines and fluid machines. The numerical methods such as finite element method (FEM) and boundary element method (BEM) are suitable to predict the acoustic attenuation performance of mufflers[1,2]. Comparing the computational complexity of FEM and BEM, BEM is the winner at the dimensionality of the problem due to its surface-only meshing scheme, but respect to the computational time, BEM handling dense matrices does not have an advantage over the FEM handling sparse or band matrices. If a direct solver for linear systems like Gaussian elimination is used, the two methods have an equal order of complexity. If an iterative solver is used and assuming that the iterations converge rapidly, the computational time of BEM still $O(N^2)$, where N is the number of unknowns. When the scale of the problems become large, the memory requirement of FEM and BEM is hard to be surported by the PCs since the huge number of nodes and too long computational time.

To overcome these shortcomings, the fast multipole algorithm (FMA) originally developed by Rokhlin[3] is employed for this difficulty, it provides an efficient mechanism for computing potential in large-scale systems and leads to an advanced boundary element method—FMBEM. FMBEM has been applied in various fields[4-5], including the acoustic problems, it has a possibility to drastically reduce the computational complexity and time in dealing with the large-scale sound field analysis.

For the interior sound field analysis, the FMBEM is maily applied to calculate the sound field with single domain and single medium (air). However, the practical mufflers usually have complex internal structures which contain perforated tubes, thin bafflers, branched cavites, extended inlet/outlet tubes. The traditional FMBEM fails to yield reliable results because the presence of singular boundaries and very fine meshes have to be used and nearly singular behavior may occur in the integral equation. In order to solve this problem, two approaches (the substructure FMBEM and the direct mixed-body FMBEM) are proposed in the present paper.

In the substructure FMBEM, the imaginary interfaces are constructed to divide the acoustic domain into several subdomains, so each domain has a well-defined bondary and the FMBEM can be employed to compute the matrix-vector products for each subdomain. Be different from the conventional substructure BEM[6], the coefficient matrix is not explicitly calculated in FMBEM, so the global matrix-vector products should be obtained by superpose the matrix-vector products of each sub-domain.

The direct mixed-body FMBEM combines the FMA with direct mixed-body BEM developed byWu etc.[7,8]. The advantage is that, the thin wall components just need to be discretized once, and no imaginary interface will be created, so it's excellent for reducing the number of unknows to be solved. The disadvantage is that the thickness of these components is neglected. If the thickness of thin walls can be ignored, the direct mixed-body FMBEM will be more suitable for the analysis of the large complex sound fields.

In the present paper, the two approaches are investigated and developed to predict the acoustic performance of mufflers with complex internal structures. As an example of application, the transmission loss of an expansion chamber with extended inlet and outlet tubes is calculated by using the substructure FMBEM and direct mixed-body FMBEM. The constant elements are used to discretize the boundaries for simplicity. Finally, the availability and accuracy of the approaches are confirmed by comparing the numerical results with the experimental data.

BASIC IDEA OF FAST MULTIPOLE METHOD

Suppose that we evaluate the set of integrals as follow over n field panels, with respect to m source points.

$$I(x_i) = \sum_{j=1}^{n} \int_{\Gamma_j} K(x_i, y)\phi(y)dS(y) \quad i = 1, \ldots, m \qquad (1)$$

With reference to Figure 1, the integrations could be performed directly (for example by using a Gauss quadrature scheme) leading to order $O(m \times n)$ computational complexity. If we apply the FMM, choosing a point y_0 near the field region and another point x_0 near the source region, the integrations can then be evaluated fast by the fast multipole algorithm. The total computational cost of the operation is thus of order $O(m + n)$.

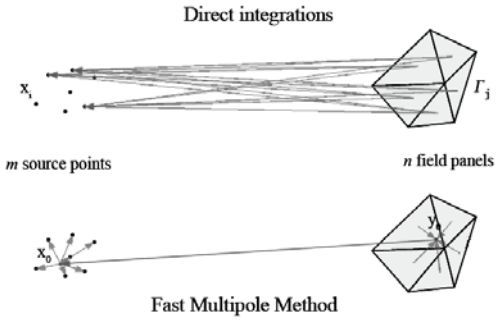

Figure 1. Scheme of basic FMM application

The key idea of fast multipole method (FMM) is that, a multipole expansion of the kernel should be build in which the connection between the collocation point and the integration point is separated, and group the discretized nodes to different sells and levels by a hierarchical structure, then according to the position relationship of the nodes, the computation of integrations can be then accelerated using the fast multipole algorithm[9].

SUBSTRUCTURE FMBEM

Fundamentals of FMBEM

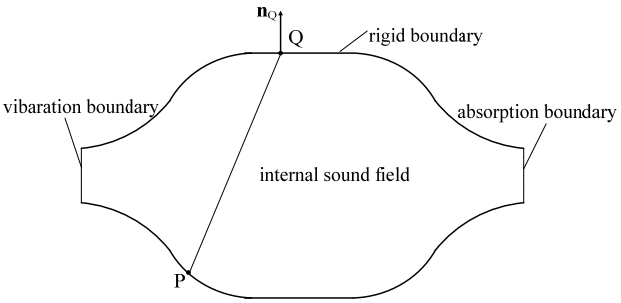

Figure 2. Internal sound field with general bondary

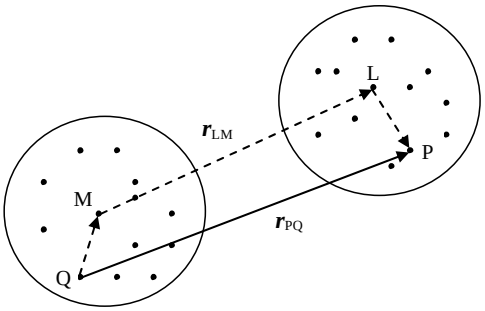

Figure 3. Geometry of the four poins

For the inernal sound field shown in Figure 2, it contains three kinds of boundaries: rigid boundary, vibration boundary and absorption boundary. The steady-state linear acoustics with the $e^{-j\omega t}$ convertion are assumed, where $j = \sqrt{-1}$. If point P is on a smooth bounary, then the sound pressure at P can be calculated by the Kirchhoff-Helmholtz boundary integral equation[10].

$$\frac{1}{2}p(\boldsymbol{r}_P) = \int_\Gamma \left(G(\boldsymbol{r}_P, \boldsymbol{r}_Q)\frac{\partial p(\boldsymbol{r}_Q)}{\partial \boldsymbol{n}_Q} - p(\boldsymbol{r}_P)\frac{\partial G(\boldsymbol{r}_P, \boldsymbol{r}_Q)}{\partial \boldsymbol{n}_Q} \right) dS \qquad (2)$$

The normal derivative of sound pressure is related to the particle normal velocity by

$$\frac{\partial p(\boldsymbol{r}_Q)}{\partial \boldsymbol{n}_Q} = -j\rho\omega v_n(\boldsymbol{r}_Q) \qquad (3)$$

where ρ is the mean density of the fluid and ω is the angular frequency. So equation (2) becomes

$$-\frac{1}{2}p(\boldsymbol{r}_P) = \int_\Gamma \left(j\rho\omega v_n(\boldsymbol{r}_Q)G(\boldsymbol{r}_P, \boldsymbol{r}_Q) + p(\boldsymbol{r}_P)\frac{\partial G(\boldsymbol{r}_P, \boldsymbol{r}_Q)}{\partial \boldsymbol{n}_Q} \right) dS \qquad (4)$$

where $\partial / \partial \boldsymbol{n}_Q$ denotes the normal derivative, and G is the Green's function given by

$$G(\boldsymbol{r}_P, \boldsymbol{r}_Q) = \exp(jkr_{PQ}) / 4\pi r_{PQ} \qquad (5)$$

Regarding each collocation point, in order to accelerate the computation of its boundary integration, the sound field has to be divided into near and far field according to the position relationship between the collocation and integration point, and then the FMM will be applied in the far field, so the kernel intergral equation should be writen as a multipole expansion. With reference to the geometry among four points in Figure 3, the Green's function is transformed into the follow expansion according to the Gegenbauer's addition theorem [11] and plane wave expansion[12].

$$G(\boldsymbol{r}_P, \boldsymbol{r}_Q) = \frac{e^{jk|r_{MQ} + r_{LM} + r_{PL}|}}{4\pi \left| \boldsymbol{r}_{MQ} + \boldsymbol{r}_{LM} + \boldsymbol{r}_{PL} \right|} = \frac{jk}{16\pi^2} \oint E_{PL}(k\hat{\boldsymbol{s}}) T_{LM}(k\hat{\boldsymbol{s}}) E_{MQ}(k\hat{\boldsymbol{s}}) \mathrm{d}\hat{\boldsymbol{s}} \qquad (6)$$

where $E_{PL}(k\hat{\boldsymbol{s}}) = \exp(jk\hat{\boldsymbol{s}} \bullet \boldsymbol{r}_{PL})$, $E_{MQ}(k\hat{\boldsymbol{s}}) = \exp(jk\hat{\boldsymbol{s}} \bullet \boldsymbol{r}_{MQ})$ (7)

$$T_{LM}(\hat{\boldsymbol{s}}) = \sum_{l=0}^{\infty} j^l (2l+1) h_l^{(1)}(kr_{LM}) P_l(\hat{\boldsymbol{s}} \bullet \hat{\boldsymbol{r}}_{LM}) \qquad (8)$$

M is the multipole expansion point, L is the local expansion point, P is a collocation point and Q is a integration point, the four points are located with the provision that $r_{PL} < r_{LM}$ and $r_{MQ} < r_{PM}$. k is the wavenumber, $\hat{\boldsymbol{s}}$ is the integration vector on the unite sphere, $h_l^{(1)}$ is the first kind of Hankel function, P_l are the Legendre polynomials. Accordingly, the normal derivative of the Green's function at q can be expressed by

$$\frac{\partial G(\boldsymbol{r}_P,\boldsymbol{r}_Q)}{\partial n_Q}=\frac{(jk)^2}{16\pi^2}\oint E_{PL}(k\hat{\boldsymbol{s}})T_{LM}(k\hat{\boldsymbol{s}})E_{MQ}(k\hat{\boldsymbol{s}})(n_Q\bullet\hat{\boldsymbol{s}})\mathrm{d}\hat{\boldsymbol{s}} \qquad (9)$$

For the multilevel translation relationship between the collocation point and integration point in the far field, the multipole expansion should be rewriten as:

$$G(\boldsymbol{r}_P,\boldsymbol{r}_Q)=\frac{jk}{16\pi^2}\oint E_{P\lambda_{mL}}(k\hat{\boldsymbol{s}})Z^I_{\lambda_{mL}\lambda_{m'L}}(k\hat{\boldsymbol{s}})E_{\lambda_{m'LQ}}(k\hat{\boldsymbol{s}})\mathrm{d}\hat{\boldsymbol{s}} \qquad (10)$$

$$\text{with } Z^I_{\lambda_{mL}\lambda_{m'L}}(k\hat{\boldsymbol{s}})=\prod_{l=I}^{L-1}E_{\lambda_{m(l+1)}\lambda_{ml}}(k\hat{\boldsymbol{s}})T_{\lambda_{ml}\lambda_{m'l}}(k\hat{\boldsymbol{s}})\prod_{l=I}^{L-1}E_{\lambda_{m'l}\lambda_{m'(l+1)}}(k\hat{\boldsymbol{s}}) \qquad (11)$$

m'L belongs to the interaction cells of the cell *mL* at the lowest level *L*, and *I* is the level number at which the interaction contributions of cells are computed. λ means the cell's center. According to the principle of cells dividing, there are no interaction cells before level 2, so the equation (10) will be adopted when $L\geqslant 3$. Regarding cells, hierarchical structure is introduced where a cubic cell circumscribing the whole boundary is determined as the root cell and is divided into child cells at the lower level in turn. At each level interactions between cells are numerically evaluated. (The full details to the concept of hierarchical cell structure and the definition of interaction cells and neighbor cells refer to [13])

Substituting equation (6) and equation (9) into equation (4), the multipole expansion connecting the collocation point and the integration point is built. All the interaction cells and neighbor cells at each level are difined based on a hierarchical cell structure. In the near field, the matrix-vector multiplication in solving the boundary integral equaton is achieved by the conventional BEM (CBEM); in the far field, the matrix-vector multiplication is achieved by the FMM. Finally, the whole matrix-vector products can be obtained by adding the two results (The full process of FMBEM refers to [13]).

Substructure technique for FMBEM

The substructure approach is widely used in the BEM analysis for the silencers with complex internal structure. However, because the coefficient matrix in FMBEM is not calculated in the explicit form, this approach is impossible to be applied directly to FMBEM in the same manner as the substructure BEM approach.

In order to apply the substructure approach to FMBEM, the whole acoustic domain is divided into two subdomains as shown in Figure 4. Discretizing the boundary of each subdomain, p_1, v_1 and p_2, v_2 denote the sound pressure and the particle velocity on the real bondary (all boundaries except the interface bounary) of subdomain Ω_1 and Ω_2 respectively; p_{12}, v_{12} and p_{21}, v_{21} denote the sound pressure and the particle velocity on the interface belong to the subdomains Ω_1 and Ω_2 respectively. This sound field contains: rigid wall boundary, vibration boundary at the inlet, absorption boundary at the outlet and continuity condition at the interface.

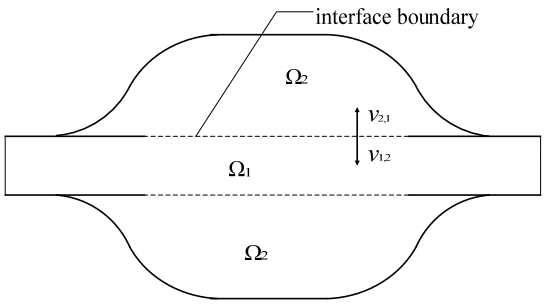

Figure 4. Division of acoustic domain

As mentioned above, the FMBEM directly yield the matrix-vector products, we can not compose the global matrix by moving the unknowns of the subdomains to the left-hand side. Here we superpose matrix-vector products calculated in each sub-domain to efficiently obtain the global matrix-vector products. In the following expression, each matrix-vector product in the global matrix-vector products can be calculated efficiently by applying the FMBEM to each sub-domain.

$$\begin{bmatrix}[\boldsymbol{H}_{11}\ \boldsymbol{H}_{12}]\begin{Bmatrix}\boldsymbol{p}_1\\ \boldsymbol{p}_{1,2}\end{Bmatrix}-[\boldsymbol{G}_{11}\ \boldsymbol{G}_{12}]\begin{Bmatrix}0\\ \boldsymbol{v}_{1,2}\end{Bmatrix}\\ [\boldsymbol{H}_{21}\ \boldsymbol{H}_{22}]\begin{Bmatrix}\boldsymbol{p}_2\\ \boldsymbol{p}_{2,1}\end{Bmatrix}-[\boldsymbol{G}_{21}\ \boldsymbol{G}_{22}]\begin{Bmatrix}0\\ \boldsymbol{v}_{2,1}\end{Bmatrix}\end{bmatrix}=\begin{bmatrix}[\boldsymbol{G}_{11}\ \boldsymbol{G}_{12}]\begin{Bmatrix}\boldsymbol{v}_1\\ 0\end{Bmatrix}\\ [\boldsymbol{G}_{21}\ \boldsymbol{G}_{22}]\begin{Bmatrix}\boldsymbol{v}_2\\ 0\end{Bmatrix}\end{bmatrix} \qquad (12)$$

on the interface, the continuity condition must be satisfied:

$$\boldsymbol{p}_{1,2}=\boldsymbol{p}_{2,1} \qquad (13)$$

$$\boldsymbol{v}_{1,2}=-\boldsymbol{v}_{2,1} \qquad (14)$$

By this way, the substructure FMBEM can handle all kinds of sound field with complex internal structure. Also, the computational complexity of this procedure can be $O(N_a\ lnN_a)$, where N_a is the sum of number of unknows on the boundary of Ω_1 and Ω_2.

DIRECT MIXED-BODY FMBEM

Idea of mixed-body

As we know about the substructure FMBEM, if a model contains many thin obstacles or if the one of the subdomains are intricately connected to another, then the zoning and matching procedure of substructure technique is usually tedious and time consuming, especially for the thin walls with big size, the substructure FMBEM will not be a wise and practical choice.

To avoid this problem, a method called direct mixed-body BEM derived from the conventional multi-domain BEM was proposed by Wu and Wan, they overcome the thin-body difficulty by using the hypersingular integral equation. In this approach, the real boundaries only need to be meshed once, and all the values on these dicretizing nodes can be governed by the mixed-body integral formulation.

Combination of FMA and direct mixed-body BEM

With reference to Figure 5, there are three kinds of boundary in the sound field, S_r, S_t and S_p denote the regular wall plus the inlet and outlet ends, the thin walls (including the inrernal connecting tubes, extended inlet/outlet tubes and thin baffles) and the perforated tubes, respectively. The unit outward normal vector on S_r is pointing away from the interior acoustic domain, the unit normal vector on S_t and S_p can be pointing to either side of the thin walls.

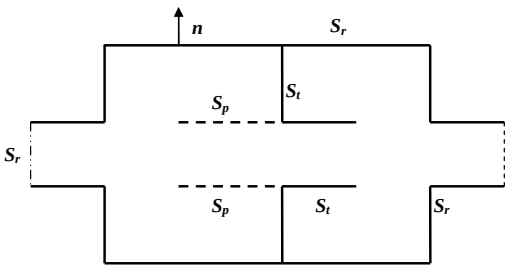

Figure 5. Boundary definition for the mixed-body approach

The multi-domain BEM is first employed to obtain several subdomains, each of which has a well-difined boundary. This will yield some imaginary interfaces. By forming a set of

subdomain boundary integral equations and adding them up, all the integrals over the imaginary interfaces are cancelled out due to the continuity condition at the imaginary interfaces[14]. Therefore, the single-domain direct mixed-body boundary integral equations are[8]

$$\int_{S_r}\left(\frac{\partial G}{\partial \boldsymbol{n}_Q}p + j\rho\omega v_n G\right)dS + \int_{S_t+S_p}\frac{\partial G}{\partial \boldsymbol{n}_Q}(p^+ - p^-)dS = -\frac{1}{2}p(P) \qquad P\in S_r \tag{15}$$

$$\int_{S_r}\left(\frac{\partial^2 G}{\partial \boldsymbol{n}_Q\partial \boldsymbol{n}_P}p + j\rho\omega v_n\frac{\partial G}{\partial \boldsymbol{n}_P}\right)dS + \int_{S_t+S_p}\frac{\partial^2 G}{\partial \boldsymbol{n}_Q\partial \boldsymbol{n}_P}(p^+ - p^-)dS = \begin{cases} j\rho\omega v_n(P) & P\in S_t \\ -\dfrac{jk}{\xi}(p^+(P)-p^-(P)) & P\in S_p \end{cases} \tag{16}$$

where P is the collocation point, G is the Green's function, ρ is the mean density of the fluid, k is the wavenumber, and ξ is the non-dimensional transfer impendance for the perforated surface S_p , $p^+$and p^- is the sound pressure on the positive side and the opposite side of the thin walls (S_t or S_p), $\partial/\partial n^p$ means partial differentiation with respect to the normal direction of P. The expression of G is

$$G = \exp(jkr)/4\pi r \tag{17}$$

where $r = |P-Q|$, Q is any integration point at the boundary. Equation (15) and (16) together form a complete set of boundary integral equations for muffler analysis. Apparently that, the direct mixed-body BEM still have a difficullty that the hypersingular integral in equation (16) needs to be regularized before mumerical implementation, there are various techniques for dealing with this problem[15-17], but lots of them have a complex implement process, and the complexity for programing will be increased.

However, the combination of FMA and direct mixed-body BEM can handle this problem naturally. In order to apply the FMM to the mixed-body approach, the multipole expansion of Green's function is used here again. Because of

$$\partial E_{MQ}(k\hat{\boldsymbol{s}})/\partial n_Q = jk(n_Q\bullet\hat{\boldsymbol{s}})E_{MQ}(k\hat{\boldsymbol{s}}) \tag{18}$$

and

$$\partial E_{PL}(k\hat{\boldsymbol{s}})/\partial n_P = jk(n_P\bullet\hat{\boldsymbol{s}})E_{PL}(k\hat{\boldsymbol{s}})\ , \tag{19}$$

the hypersingular kernels used in equation (16) are transformed into the multipole expansion as follow:

$$\frac{\partial^2 G}{\partial n_Q\partial n_P} = -\frac{jk^3}{16\pi^2}\oint E_{PL}(k\hat{\boldsymbol{s}})T_{LM}(k\hat{\boldsymbol{s}})E_{MQ}(k\hat{\boldsymbol{s}})(n_Q\bullet\hat{\boldsymbol{s}})(n_P\bullet\hat{\boldsymbol{s}})\mathrm{d}\hat{\boldsymbol{s}} \tag{20}$$

So it is ideally suitable to mixed-body BEM for combining with the FMA. The same as the FMBEM, substituting equations (9) and (20) into equations (15) and (16), the multipole expansion connecting the collocation point and the integration point can be formed. Also, by discretizing the mixed-body boundary integral equation, the matrix-vector products are solved using the mixed-body BEM and FMM in the near and far fields respectively. The matrix form of the combined equations (15, 16) is

$$\begin{bmatrix} H_{rr} & H_{rt} & H_{rp} \\ H_{tr} & H_{tt} & H_{tp} \\ H_{pr} & H_{pt} & H_{pp} \end{bmatrix}\begin{Bmatrix} p \\ p^+ - p^- \\ p^+ - p^- \end{Bmatrix} = \begin{Bmatrix} b_r \\ b_t \\ b_p \end{Bmatrix}, \tag{21}$$

the first row is generated by equation (15), the second and the third row by equation (16); the first subscript of each sub-matrix refers to the position of the collcation point P, and the second subscript refers to the position of the unknown nodes.

It should be noted that, the governing equations (15) and (16) consist of two integral equations with defferent integral domain, so considering the application of FMM in the far field, when we divide the nodes into defferent cells and levels, the nodes located on the regular boundaries and thin bondaries have to be grouped separately.

NUMERICAL EXAMPLE

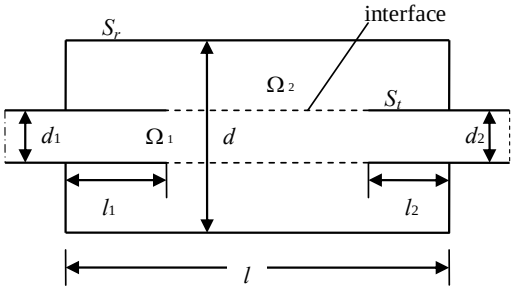

Figure 6. Circular expansion chamber with extended inlet and outlet tubes

A circular expansion chamber with extended inlet and outlet tubes shown in Figure 6 is considered, the dimensions are: d_1=d_2=0.0486m, d=0.1532m, l_1=0.08m, l_2=0.04m, l=0.2823 m. In order to apply the the substructure FMBEM, the acoustic domain is divided into two subdomains. For the employment of the direct mixed-body FMBEM, we set two kinds of boundary (S_r and S_t). The two approaches are applied to calculate the transmission loss of the muffler. All the computations are conducted on a desktop PC with an Intel Pentium 4 processor 2.93GHz and 2G of memory.

We set a unit amplitude velocity at the inlet, and the anechoic condition (characteristic impedance condition) at the outlet, then transmission loss of the muffler may be determined by using the follwing expression:

$$TL = 20\log\left|\frac{p_i + \rho c v_i}{2p_o}\right| + 10\log\left|\frac{S_i}{S_o}\right| \tag{22}$$

where p_i, v_i is the sound pressure and particle velocity on the inlet surface, respectively, p_o is the sound pressure on the outlet surface, c is the speed of sound , S_i and S_o are the areas of inlet and outlet of the muffler respectively.

The transmission loss (TL) of the reactive silencer calculated by substructure FMBEM and direct mixed-body FMBEM is shown in Figure 7, and the numerical results are verified by comparing with the experimental data[18]. Figure 8 shows the total computational time of three methods at 500Hz, versus number of nodes. It may be seen that, compared to the BEM, the advantage of FMBEM in reducing computational time is more obvious as the number of nodes increasing, also, this figure shows the similar computational efficiency of substructure FMBEM and direct mixed-body FMBEM in solving the same number of equations. However, it can not be ignored that, the direct mixed-body FMBEM can reduce the amount of discretized nodes because of its thin components meshing once only without adding imaginary interface. So, if the total time is displayed versus the length of meshes as shown in Figure 9, it is clear that the direct mixed-body

FMBEM can create less meshes than substructure FMBEM at each length for the same model, so the direct mixed-body FMBEM may save the computational time when the size of meshes becomes smaller.

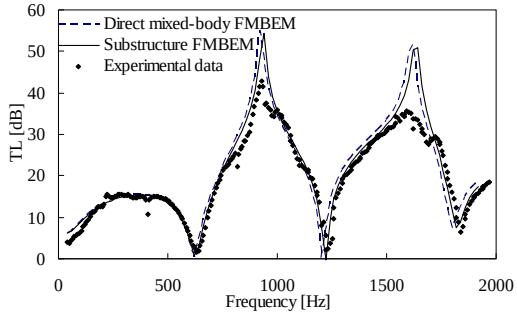

Figure 7. Transmission loss of expansion chamber with extended inlet and ourlet

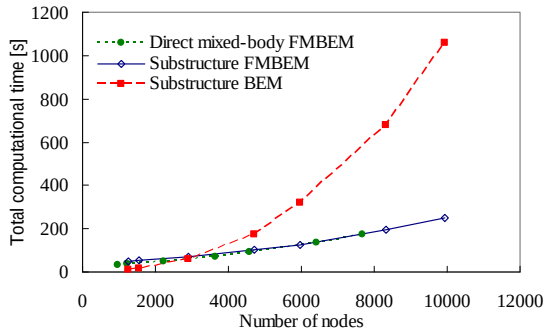

Figure 8. Total computational time versus number of nodes

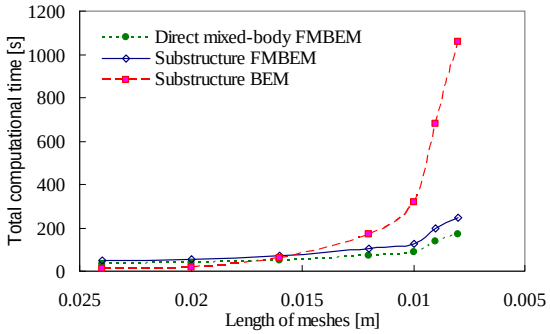

Figure 9. Total computational time versus length of meshes

CONCLUSIONS

The substructure FMBEM and direct mixed-body FMBEM are investigated and developed to overcome the thin wall dificullty in the internal sound field computation. The availability and accuracy of the two approaches are confirmed by comparing the TL of a reactive silencer with the experimental data. When the number of unknows is big, they also have an obvious advantage to CBEM in saving the computational time.

Comparing the substructure FMBEM, the direct mixed-body FMBEM is more suitable for solving the problem with many thin walls, and may save more computational time than the substructure FMBEM when its number of nodes on interface and thin walls gets bigger. However, if the thickness of thin wall can not be neglected, the mixed-body FMBEM is not suitable. So the substructure FMBEM have a good applicability in solving the internal sound field with any shape geometry.

ACKNOWLEDGEMENT

The authors acknowledge the support of the research grant 10874034 from National Natural Science Foundation of China, and the first author would like to thank Prof. Z.L. Ji and Dr. P.J. Ming for their guidance and helpful discussions.

REFERENCES

1 B.B. Xu, Z. L. Ji, “Finite element analysis of acoustic attenuation performance of perforated tube silencers” *Journal of Vibaration and Shock* (in chinese). **28**(9), 112-115 (2009)
2 Z. L. Ji, A. Selamet, “Boundary element analysis of three-pass perforated duct mufflers” *Noise Control Engineering Journal.* **48**(5), 151-156 (2000)
3 Rokhlin V, “Rapid solution of integral equations of classical potential theory” *Journal of Computional Physics*. **60**, 187-207 (1983)
4 N. Nishimura, “Fast multipole accelerated boundary integral equation methods” *American Society of Mechanical Engineers*. **55**(4), 299-324 (2002)
5 X.R. Wang, Z. L. Ji, “Fast multipole acoustic BEM and its application” *Journal of Harbin Engineering University* (in chinese). **28**(7), 752-757 (2007)
6 Z. L. Ji, “Acoustic attenuation performance prediction and analysis of perforated tube dissipative silencers” *Journal of Vibration Engineering*. **18**(4), 453-457 (2005)
7 T.W. Wu, C.Y.R. Cheng, P. Zhang, “A direct mixed-body boundary element method for packed silencers” *J. Acoust. Soc. Am*. **111**(6), 2566–2572 (2002)
8 T.W. Wu, G.C. Wan, “Muffler performance studies using a direct mixed-body boundary element method and a three-point method for evaluating transmission loss” *Journal of vibration and Acoustics*. **118**, 479–484 (1996)
9 J. Board, K. Schulten, “The fast multipole algorithm” *IEEE Comput. Sci. Eng*. **2**(1), 76–79 (2000)
10 A.D. Pierce, *Acoustics: an introduction to its physical principles and applications* (McGraw-Hill, New York, 1981)
11 M. Abramowitz, I.A. Stegun, *Handbook of Mathematical Functions* (Dover, New York, 1965)
12 V. Rokhlin, “Diagonal forms of translation operators for the Helmholtz equation in three dimensions” *Applied and Computational Harmonic Analysis*, **1**(1), 82-93 (1993)
13 T. Sakuma, Y.Yasuda, “Fast multipole boundary element method for large-scale steady-state sound field analysis. part I: Setup and Validation” *Acta Acustica united with Acustica*, **88**, 513-525 (2002)
14 T.W. Wu, G.C. Wan, “Numerical modelling of acoustic radiation and scattering from thin bodies using a Cauchy principal integral equation” *J. Acoust. Soc. Am*. **92**(5), 2900–2906 (1992)
15 G. Krishnasamy, L.W. Schmerr, T.J. Rudolphi etc. “Hypersingular boundary integral equations: some applications in acoustic and elastic wave scattering” *ASME J. Appl. Mech*. **57**, 404-414 (1990)
16 X.F. Wu, A.D. Pierce, J.H. Ginsberg, “Variational method for computing surface acoustic pressure on vibrating bodies, applied to transversely oscillating disks” *IEEE J. Oceanic Eng*. **12**, 412-418 (1987)
17 Y.J. Liu, S.H. Chen, “A new form of the hypersingular boundary integral equation for 3-D acoustics and its implementation with C^0 boundary elements” *Comput. Methods Appl. Mech. Engrg*. **173**, 375-386 (1999)
18 A. Selamet, Z. L. Ji, “Acoustic attenuation performance of circular expansion chambers with extended inlet/outlet” *Journal of Sound and Vibration*. **223**(2), 197-212 (1999)